JPET Fast Forward. Published on December 20, 2017 as DOI: 10.1124/jpet.117.244400
This article has not been copyedited and formatted. The final version may differ from this version.

A combination of chitosan, cellulose and seaweed polysaccharide inhibits postoperative intra-abdominal adhesion in rats

Authors
Lin Tian, Huan Li, Yan Li, Kun Liu, Yao Sun, Zhongcheng Cong, Xue Luan, Yao Li, Jinglin Chen, Lin Wang, Zhihui Ren, Dengli Cong, Haotian Wang, Jin Pei

Author Affiliations
School of Pharmaceutical Sciences, Jilin University, Changchun, Jilin, China

a) Running title : CCS Prevents postoperative intra-abdominal adhesion

b) Corresponding Author :
Jin Pei，
School of Pharmaceutical Sciences,Jilin University, Jilin 130000, China.
E-mail: peijin@jlu.edu.cn
Telsphone:+8613843171367
Fax:+86-043185619252

c) The number of text pages:32

The number of tables: 1

The number of figures：10

The number of references：45

The number of words in the Abstract：177

The number of words in the Introduction：369

The number of words in the Discussion:1464

d) Nonstandard abbreviations:

tPA,tissue plasminogen activator; PAI-1,plasminogen activator inhibitor-1; TGF-β1, transforming growth factor β1; TNF-α, tumor necrosis factor-a; JNK, c-Jun N-terminal kinase; TAK1,transforming growth factor–activated kinase 1; ERK,extracellular regulated protein kinases ; YAP/TAZ, Yes-associated protein/ transcriptional coactivator with PDZ-binding motif ; RhoA/ROCK, Ras homologue protein/Rho associated coiled coil forming protein.

Recommended section assignment: Drug Discovery and Translational Medicine

JPET Fast Forward. Published on December 20, 2017 as DOI: 10.1124/jpet.117.244400
This article has not been copyedited and formatted. The final version may differ from this version.

Abstract

Intra-abdominal adhesion is a common complication after laparotomy. Conventional therapeutic strategies still cannot safely and effectively prevent this disorder. In this study, a combination of chitosan, cellulose and seaweed polysaccharide (CCS) was developed to significantly alleviate the formation of postoperative adhesion in rats with abdominal trauma. Transforming growth factor beta-1 (TGF-β1, an important promoter of fibrosis) and its downstream factors namely alpha-smooth muscle actin (α-SMA) and plasminogen activator inhibitor-1 (PAI-1) were effectively suppressed by CCS *in vivo* and as a result, the activation of tissue plasminogen activator (tPA, may generate plasmin that is a fibrinolytic factor capable of breaking down fibrin) was significantly promoted, presenting anti-fibrosis effects of CCS. In addition, the activity of kinases (e.g. TAK1, JNK/SAPK and p38) in mitogen-activated protein kinase (MAPK) inflammation signaling pathway was also significantly suppressed by CCS *in vivo*, demonstrating anti-inflammatory functions of CCS. The histological studies further confirmed the role of CCS in the inhibition of the fibrosis, collagen deposition, inflammation, and vascular proliferation. These results indicate the clinical potential of CCS in the treatment of postoperative intra-abdominal adhesion.

Introduction

Postoperative intra-abdominal adhesion is a common complication found in 90% to 95% of patients undergoing abdominal surgery (Yang et al., 2012; Hu et al., 2015). The intra-abdominal adhesions do not only affect intestinal motility of patients, also cause the abdominal pain, intestinal obstruction, intestinal necrosis, and other discomforts (Deng et al., 2016; Poehnert et al., 2016). Good surgical technique (e.g. the avoidance of extensive surgical incisions and the use of microtraumatic/atraumatic suture materials) may minimize serosal injury and therefore decrease adhesion formation. (Risberg, 1997; Liakakos et al., 2001). However, surgical technique alone cannot prevent de novo formation and particularly reformation of abdominal adhesions. Adjuvant therapeutic strategies to suppress the adhesion formation after peritoneal injuries comprise two categories: 1) barriers (a medical implant that may reduce adhesions following surgery) are used to separate serosal surfaces during the early stages of wound repair and therefore inhibit the coagulation, fibrin deposition, and fibroblastic activity. Barriers have been studied clinically to decrease the frequency and severity of postoperative adhesion formation (Parsak et al., 2007); 2) medicines are used to alter the adhesion-induced inflammatory signaling pathways, as a result suppressing the inflammatory process (e.g. infection, endotoxin and exudation) (Gomel et al., 1996). However, no treatment has been widely accepted to safely and effectively prevent postoperative intra-abdominal adhesions, and therefore, novel strategies are highly required.

Chitosan, the *N*-deacetylated derivative of chitin, has been used following intestinal surgery to promote tissue repair and avoid tissue adhesion (Francesko and Tzanov, 2011). Cellulose as a barrier can effectively separate the injured tissues, therefore reducing the secretion of collagen and proliferation of fibroblast locally (Lou et al., 2012). Seaweed polysaccharides have been used as the adjuvant therapeutic material to reduce the adhesion formation (Rocha et al., 2001). In this study, the

co-administration of chitosan, cellulose and seaweed polysaccharide (CCS) was performed in rats with abdominal surgery, and as a result, CCS significantly alleviated the intra-abdominal adhesion when compared to the treatment of chitosan (CS), cellulose (CL) and carboxymethyl chitosan (CC, a derivative of chitosan widely used as the anti-adhesion agent). In addition, the anti-fibrosis and anti-inflammation mechanisms of CCS were also confirmed *in vivo*. Consequently, CCS holds great therapeutic potential in the treatment of postoperative intra-abdominal adhesion.

Materials and Methods

Animals

Male Wistar rats (220 g to 250 g) were used in this study. Animals were housed under standard laboratory conditions at a constant room temperature (RT) for at least 7 d before experiments. Rats were deprived of food for 12 hr but had free access to water before experiments. Animal works were reviewed and approved by the Animal Care and Use Committee of the Jilin University.

Reagents

Chitosan (CS), cellulose (CL), seaweed polysaccharides (SP) and carboxymethyl chitosan (CC) were purchased from Sinopharm Pharmaceutical Co., Ltd, China. As described in manufacturer's instructions, the polymeric level of CS was 2000 to 2100 with 70 percent deacetylation, the degree of polymerization of CL was 215 to 240, and the polymerization degree of seaweed polysaccharide (it is extracted from brown seaweed) was 500. The aforementioned materials were directly used as advised by suppliers. In addition, the other reagents were purchased from Sigma-Aldrich, unless specially mentioned.

5 mg CS, 3 mg CL and 1.5 mg SP were dissolved in 1 ml sterile phosphate-buffered saline (PBS) to prepare CCS. In addition, CS (10 mg/ml) and CL (6 mg/ml) were prepared for anti-adhesion studies, respectively. It is worth noting that SP as an adjuvant material can increase the viscosity of CCS, but the effect of this component alone on the prevention of postoperative adhesion was mild (Rocha et al., 2001). Therefore, SP alone was not used in this work. In addition, CC is a non-toxic derivative of chitosan generated by carboxymethylation reaction (70%) (Mn = 3 KD), and has been widely investigated in the treatment of intra-abdominal adhesion (Ryan and Sax, 1995). Therefore, CC (8 mg/ml, PBS) was used as the positive control in this study.

Experimental Design and Operative Procedure

Animals were anesthetized by intraperitoneal injection with chloral hydrate (10%) at a concentration of 0.3 ml per 100 g body weight. Rats with intra-abdominal adhesion (the model group) were prepared as described in (Zhang et al., 2014). Briefly, the cavum abdominis was accessed followed by a 2 cm to 3 cm abdominal midline incision, and the pouch-like cecum was exposed to the air for approximately 5 min. The cecum wall and its opposite parietal peritoneum were abraded mildly by the scalpel blade until the punctate hemorrhage was observed. In addition, the untreated group (without surgery) and the sham group (only with abdominal midline incision) were also prepared.

The doses of the compounds and their combination used in this study were first determined using healthy Wistar rats. On four hours following intraperitoneal injection of the compounds and their combination, IFN-alpha, IL-6 and IL-12 in the serum were analyzed using ELISA kits (Nanjing Jiancheng Bioengineering Institute, Nanjing, Jiangsu, China) according to the manufacturer's instructions. No acute immunological response was caused using the doses mentioned below (data not shown).

At the time of surgery, the model group was treated using CCS with low, middle, and high doses (mg compound per kg body weight):

Low dose: 20 mg/kg CS + 12 mg/kg CL + 9 mg/kg SP

Middle dose: 40 mg/kg CS + 24 mg/kg CL + 12 mg/kg SP

High dose: 60 mg/kg CS + 36 mg/kg CL + 18 mg/kg SP

In addition, 2 ml saline, 80 mg/kg CS, 48 mg/kg CL and 32 mg/kg CC were administrated into the abdominal cavity of the model group, respectively.

Animals were maintained for 14 d and the body weight was recorded regularly to further determine the toxicity.

Adhesion Grade and Assessment

On Day 14 following the surgery, animals were anesthetized by intraperitoneal injection with chloral hydrate (10%) at a concentration of 0.3 ml per 100 g body weight. The abdominal wall was opened with an inverted "U" shape incision. The adhesion was evaluated by the adhesion grade criteria reported in (Nair et al., 1974), as follows: 0, complete absence of adhesion; 1, single band of adhesion, between viscera or from viscera to abdominal wall; 2, two bands, either between viscera or from viscera to abdominal wall; 3, more than 2 bands, between viscera or viscera to abdominal wall or whole intestines forming a mass without being adherent to abdominal wall; 4, viscera directly adherent to abdominal wall, irrespective of number and extent of adhesive bands. The researchers who assessed the grade were independent and were blinded to the design.

Enzyme-Linked Immunosorbent Assay (ELISA)

Blood was collected from the animal eyeballs, coagulated for 20 min at RT, and centrifuged at 3,000 rpm for 10 min. The serum TNF-α, TGF-β1, tPA and PAI-1 were evaluated using ELISA kits (Nanjing Jiancheng Bioengineering Institute, Nanjing, Jiangsu, China) according to the manufacturer's instructions.

Western Blot

Total protein was extracted from the cecum and its opposite parietal peritoneum using RIPA buffer [50 mM Trish-HCl (pH = 7.4), 150 mM NaCl, 1% Triton-100, 1% Sodium Deoxycholate, 0.1% Sodium Dodecyl Sulfate (SDS), 1 mM Sodium Orthovanadate, 1 mM Sodium Fluoride, 1 mM EDTA] containing 1 mM phenylmethanesulfonyl fluoride (PMSF) (Beyotime, China) (Guo et al., 2017) .Protein concentrations were measured using the BCA Protein Assay kit (GenStar, China). 20 μg proteins were loaded into the 12% SDS-PAGE gel and electrophoresed at 80 V for 30 min. Protein was then transferred to PVDF membranes

at 120 V for 80 min. The membranes were blocked with 5% bovine serum albumin (BSA) and then incubated with antibodies (anti-TAK1 antibody, ab109526, Abcam, UK, 1:2,000; anti-JNK/p-JNK antibodies, ab17946/ab4821, Abcam, UK, 1:2,000; anti-ERK/p-ERK antibodies, ab196883/ab214362, Abcam, UK, 1:2,000/1:1,000; anti-P38/p-P38 antibodies, ab170099/ab4822, Abcam, UK, 1:2,000/1:1,000; anti-β-actin antibody, ab8226, Abcam, UK, 1:2,000; anti-pTAK1 antibody, ENP0424,Elabscience Biotechnology, China, 1:1,000; anti-α-SMA antibody, ENT5053, Elabscience Biotechnology, China, 1:1,000) overnight. Antibody reactive bands were detected using a Bio-imaging system (Micro Chemi 4.2, Israel). Densitometry analysis of bands was performed using ImageJ, and all results were normalized to β-actin control.

RT-qPCR

Total RNA was collected from the cecum and its opposite parietal peritoneum using the TransZol Up Reagent (ET111-01, TransGen Biotech, China). First-strand cDNA was generated using the TransScript All-in-One First-Strand cDNA Synthesis SuperMix for qPCR Kit (AT341, TransGen Biotech, China). Gene expression was evaluated by real-time quantitative PCR (qPCR) with the TransStart Top Green qPCR SuperMix Kit (AQ131, TransGen Biotech, China) using the Applied Biosystems Real Time PCR System (Step One Plus). The PCR reactions were carried out by 40 cycles of denaturation at 94 ℃ for 5 s and annealing at 60 ℃ for 30 s. The quantitative level of each target mRNA was measured as a fluorescent signal corrected according to the signal for GAPDH mRNA. The $2^{-\triangle\triangle}$Ct method was used to quantify the relative changes in mRNA (Guo et al., 2012).

The PCR primer sequences were as follows: TGF-β1, 5'-CAT TGC TGT CCC GTG CAG A-3' (forward) and 5'-AGG TAA CGC CAG GAA TTG TTG CTA-3' (reverse); TNF-α, 5'-AGG AGG TGC TCT CCG AGA AA-3' (forward) and 5'-TGA GGG CAT TGG CAT ACG AG-3' (reverse); tPA: 5'-CGC TGT ACC TCA CAG CAT CTG TTT

A-3' (forward) and 5'-CAT CCG CTT ATC GAT CAT GCA C-3' (reverse); PAI-15'-ACC ATC TCC GTG CCC ATG A-3' (forward) and 5'- GGG CAG TTC CAG GAT GTC GTA-3' (reverse); GAPDH: 5'-ACC ACA GTC CAT GCC ATC AC-3' (forward) and 5'- TCC ACC ACC CTG TTG CTG TA-3' (reverse).

Histological studies

Tissues from the surgical areas were fixed with 4% paraformaldehyde (PFA) at RT, dehydrated in 70%, 80%, 90% and 100% ethanol (v/v), cleaned in Xylene, and embedded in paraffin. Tissue sections (5 μm) were stained using hematoxylin and eosin (H & E) in order to assess the inflammation and vascular proliferation. In addition, Masson Trichrome kits (G1340, Solarbio Science & Technology, China) and Picrosirius Red kits (G1470, Solarbio Science & Technology, China) were used to assess the collagen deposition. Data were analyzed using the image acquisition and analysis system (Olympus Imaging, Japan).

Tissue sections (5 μm) following the antigen restoration were also incubated with 3% hydrogen peroxide (H_2O_2) solution at RT for 10 min, followed by the incubation with TGF-β1antibody (ab25121, Abcam, UK) at 4℃ overnight. Tissue sections were then incubated 15 min within the MaxVision reagent (Maxim, Fuzhou, China) for visualization, and hematoxylin was used as the counterstain. Data were analyzed using the image acquisition and analysis system (Olympus Imaging, Japan).

Statistical Analysis

The SPSS 15.0 software (SPSS, Chicago, IL, USA) was used for statistical analysis. Adhesion scores between different groups were analyzed using the Kruska-Wallis H test and the Mann-Whitney U test. Data were expressed as the median.

In addition, one-way ANOVA was applied to test the significance of differences in three or more groups using Prism version 5 (GraphPad Software Inc., San Diego, CA, USA). Data were expressed as the mean ± standard deviation. In all cases, the significance level was set at $P < 0.05$.

Results

CCS suppressed the intra-abdominal adhesion in rat model

The anti-adhesion effects of CCS were evaluated using Nair's scoring system in rats with abdominal surgery (n = 10) (Nair et al., 1974). On Day 14 following the surgery, results of Fig. 1 and Table 1 showed that no obvious abdominal adhesion was found in the untreated group (score = 0) and the sham group (score = 0). In contrast, filamentary adhesions (indicated by red triangles) were clearly found in the model group treated with saline (score = 4), which was similarly to data received in the model group without any treatment (data not shown) (the results of the model group without any treatment were not shown for the following experiments, due to the similarity to the model group with saline treatment). When compared to the model group treated with saline, CCS with low dose (score = 2.5) and middle dose (score = 2) significantly ($p < 0.05$) reduced the adhesion formation, which was similarly to data achieved by chitosan (CS, score = 2.5) and cellulose (CL, score = 2) but significantly better than results obtained by carboxymethyl chitosan (CC, score = 3). It is worth noting that CCS with high dose achieved a significant improvement (score = 2, $p < 0.01$) when compared to CCS with low and middle doses, and also demonstrated a significantly better therapeutic effect ($p < 0.05$) than CS, CL and CC. The results showed that CCS in high dose was able to effectively prevent intra-abdominal adhesion formation in rats.

The anti-adhesion properties of CCS were associated with reduction of collagen disposition, inflammation, and angiogenesis

The formation of external collagen fibrils in the cecum serosa was detected using Masson Trichrome kits(Wei et al., 2017) (Fig. 2). In Fig. 2, the level of external collagen fibers (stained in blue within the red square) in the model group treated with saline was remarkably higher than the untreated and sham groups (no obvious blue

staining). Although CS, CL and CC presented the formation of collagen fibers (stained in blue within the red square), the levels of collagen disposition were significantly less than that of the model group treated with saline (Fig.2). In addition, CCS with various doses significantly reduced the formation of collagen fibers, and more importnatly, no obvious blue staining was observed in CCS with middle and high doses, demonstrating a better therapeutic effect when compared to CS, CL and CC (Fig.2).

The formation of collagen fibrils in the cecum serosa was further evaluated using Picrosirius Red kits (Bi et al., 2017) (Fig. 3). The external collagen fibers in the injured peritoneum were stained in red as indicated within the black square. Results of Fig. 3 were similarly to those obtained using Masson Trichrome kits (Fig. 2), further confirming the prevention effect of CCS on the adhesion formation, particularly in middle and high doses.

In addition, the inflammation and angiogenesis within the cecum serosa were assessed in terms of tissue morphology using hematoxylin and eosin (H & E) staining (Fig. 4). In comparison with the untreated and sham groups, the cecum serosa was clearly damaged in the model group treated with saline due to the identification of plasma cells, granulocytes, and macrophages (shown in black square) (Fig. 4), which was similarly to results reported in(Zhang et al., 2014). In addition, CS, CL, CC and CCS (low dose) did not inhibit the induction of inflammation (shown in black square). In contrast, CCS with middle and high doses significantly inhibited the inflammatory responses, which was similar to results found in the untreated and sham groups (Fig. 4). In addition, vascular proliferation was also observed by CC (indicated by red circle), which was similar to the model group treated with saline (Fig. 4).

Results of Fig. 2, 3 and 4 indicated that the anti-adhesion properties of CCS were associated with reduction of collagen disposition, inflammation, and angiogenesis.

CCS suppressed the production of TGF-β1, α-SMA and PAI-1 and enhanced the activation of tPA

Transforming growth factor beta-1 (TGF-β1) is known to promote tissue fibrosis (Holmdahl et al., 2001). The mRNA level of TGF-β1 in rat cecum was first assessed using RT-qPCR (Fig. 5A). As shown in Fig. 5A, The TGF-β1 mRNA was significantly increased (~ 7 folds) in the model group treated with saline compared to the untreated and sham groups. Although CCS with various doses could not fully inhibited the expression of TGF-β1 mRNA (~ 3 folds), they significantly decreased the level of TGF-β1 mRNA compared to CS, CL and CC (no less than 4 folds) (Fig. 5A). In addition, the protein level of TGF-β1 was also assessed using ELISA (Fig. 5B). Interestingly, the expression of TGF-β1 protein achieved by CCS with three doses was similar to those in the untreated and sham groups, but was significantly lower than those in CS, CL and CC groups (Fig. 5B). The expression of TGF-β1 was also evaluated using immunohistochemical (IHC) staining (Fig. 6). TGF-β1 protein was clearly stained (indicated in red square) in groups of CS, CL and CC, but with less extent compared to the model treated with saline. In contrast, CCS with three doses significantly inhibited the TGF-β1 expression, which was similarly to data found in the untreated and sham groups (Fig. 6, indicated by red arrows). These results presented that CCS could significantly suppressed the production of TGF-β1 in injured cecum.

The expression of two TGF-β1 downstream factors, fibroblast marker alpha-smooth muscle actin (α-SMA) (Fig. 7) and plasminogen activator inhibitor-1 (PAI-1) (Fig. 8), was also assessed in injured cecum using RT-qPCR, western blot, and ELISA. Results in Fig. 7A and 7B demonstrated that CCS with three doses significantly reduced the protein level of α-SMA (~ 1 fold), demonstrating a better inhibitory effect compared to CS, CL and CC (~ 2 folds). In addition, the mRNA and protein levels of PAI-1 in three CCS groups were also significantly reduced compared to results found in CS,

CL and CC groups (Fig. 8A and 8B). These results demonstrated that CCS was also able to significantly suppress the production of TGF-β1 downstream factors in injured peritoneum.

Tissue plasminogen activator (tPA, can generate plasmin to break down collagen fibers) is negatively regulated by PAI-1 (Yang et al., 2008). Following the downregulation of PAI-1 (Fig. 8A and 8B), as a result, the expression of tPA was significantly enhanced by CCS with various doses (Fig. 8C and 8D), and more importantly, CCS, compared to CS, CL and CC, demonstrated a better tPA activity (Fig. 8C and 8D).

CCS was also able to inhibit the production of TNF-α and the phosphorylation of TAK1, JNK/SAPK and p38 in MAPK inflammation signaling pathway.

It is known that TGF-β1 and the inflammatory cytokine TNF-α are both the stimuli to trigger the mitogen-activated protein kinase (MAPK) inflammatory signaling pathway (Ko et al., 2016). As the expression of TGF-β1 was suppressed by CCS (Fig. 5), the downregulation of TNF-α was also investigated *in vivo* using RT-qPCR and ELISA (Fig. 9). It was clearly demonstrated that CCS also significantly reduced the expression of TNF-α mRNA and protein compared to CS, CL and CC (Fig. 9).

The activity of classic kinases in the MAPK signaling pathway such as TGF-β1-activating kinase (TAK1), c-Jun N-terminal kinase (JNK), and P38 mitogen-activated protein kinase (p38), was examined *in vivo* using ELISA (Fig. 10). Results of Fig. 10A, 10B, 10D and 10F showed that the expression of TAK1, JNK and p38 was not affected following treatments. However, as TGF-β1 and TNF-α were both suppressed, it was not surprising to note that the activity (phosphorylation) of TAK1, JNK and p38 was significantly impaired by CCS in three doses, and CCS demonstrated significantly less induction of these kinases compared to CS, CL and CC (Fig. 10A, 10C, 10E and 10G)

Taken together, the prevention efficacy of CCS (particularly with high dose) on intra-abdominal adhesion in rats (Fig. 1 and Table 1) was mainly due to two aspects: 1) anti-fibrosis effects; CCS presented significantly higher inhibitory effect on the expression of TGF-β1, α-SMA and PAI-1 (Fig. 5, 7, 8A and 8B) and therefore achieved significantly better tPA activity (Fig. 8C and 8D) and 2) anti-inflammatory effects; CCS could significantly suppress the MAPK signaling pathway (Fig. 9 and 10). These results indicated the clinical potential of CCS in the treatment of postoperative intra-abdominal adhesion.

Discussion

It is known that many of natural materials are widely used in biomedical applications, as they have biocompatible, degradable, and non-immunogenic properties. For instances, chitosan (CS) and its derivatives have been investigated as anti-adhesion materials due to the bi-function of separating tissue surfaces during the healing process and modulating the function of inflammation cells (Zhu et al., 2015). In addition, modified celluloses (CL) have been reported to gel after being placed at the injured sites, form the barriers to separate the traumatized tissue surfaces, and dissolve in the body once the tissues heal (Shao et al., 2017). Furthermore, seaweed polysaccharides (SP) as an adjuvant material have been applied for wound healing (Sanjeewa et al., 2016). Therefore, a combination of CS, CL and SP (CCS) was developed with a hope of facilitating both anti-fibrosis and anti-inflammatory effects on intra-abdominal adhesion in rats (Fig. 11).

Results of Fig. 1 and Table 1 confirmed that the adhesion formation between the injured surface and peritoneum in rats was significantly inhibited following the treatment of CCS with high dose at the time of surgery. Carboxymethyl chitosan (CC), a derivative of chitosan created by carboxymethylation reaction, retains the therapeutic effects of chitosan and has been used as biological barriers/anti-inflammatory agents to prevent the adhesion (Daroz et al., 2008). It was interesting to note that CCS with three doses presented significantly better anti-adhesion effects in comparison with CC (considered as a positive control in this study) (Fig. 1 and Table 1). The reason that CC did not reduce the adhesion formation as expected, is most likely due to the experimental conditions used in this study. In addition, the inhibitory effect achieved by CCS in high dose was also significantly greater than those obtained by CS and CL (Fig. 1 and Table 1) (SP was not used here as single treatment, as the anti-adhesion effects of this compound alone was mild (Chaturvedi et al., 2014)). These results suggested that CCS was able to effectively prevent intra-abdominal adhesion formation in rats.

The mechanistic studies of CCS as the barrier on prevention of peritoneal adhesion were first investigated using surgical rats. It is known that TGF-β1, as the main factor to promote tissue fibrosis and adhesion formation, may synthesize the fibronectin and proteoglycan for the production of collagen and extracellular matrix (ECM) (Ko et al., 2016) (Wei et al., 2015). It has been reported that the level of TGF-β1 in adhesion tissues was significantly higher than that in normal peritoneal tissues (Chang et al., 2000; Holmdahl et al., 2001), and downregulation of TGF-β1 reduced the formation of peritoneal adhesions (Zheng et al., 2013).In this study, the expression of TGF-β1 mRNA and protein was significantly inhibited by CCS *in vivo* when compared to CS, CL and CC (Fig. 5). Immunohistochemical (IHC) observation also presented that CCS achieved downregulation of TGF-β1 (Fig. 6). One of TGF-β1 downstream factors, alpha-smooth muscle actin (α-SMA) is an important fibroblast biomarker often identified in the injured tissues(Wei et al., 2017) . Western blot results in Fig. 7 showed that the α-SMA protein was also effectively downregulated in three CCS groups.

It is known that the deposition of fibrin is induced by plasminogen activator inhibitor-1 (PAI-1, one of TGF-β1 downstream factors) causing the adhesion formation (Aarons et al., 2007; Esposito et al., 2013). It has been reported that the downregulation of PAI-1 gene mediated by RNA interference (RNAi) in rats could prevent the abdominal adhesion (Chegini et al., 2001). In this study, the high expression of PAI-1 was found in the model group, and in contrast, levels of PAI-1 mRNA and protein were dramatically reduced by CCS with various doses (Fig. 8A and 8B), supporting anti-adhesion effects as observed in results of Fig. 1 and Table 1.

As tissue plasminogen activator (tPA) is negatively regulated by PAI-1, downregulation of PAI-1 may enhance the expression of tPA (Yang et al., 2008; Fotiadis et al., 2015; Honjo et al., 2017). Indeed, the levels of tPA mRNA and protein were significantly increased following CCS treatments (Fig. 8C and 8D), which was

mostly like to due to the suppression of PAI-1 (Fig. 8A and 8B). It is also known that the degradation of fibrin is improved by plasmin (a fibrinolytic factor, can break down collagen fibers) (Cassidy et al., 2014), and the generation of plasmin was enhanced by tPA (Reed et al., 2004). As shown in Fig. 1 and Table 1, the intra-abdominal adhesions were significantly reduced in surgical rats treated using CCS with three doses. Therefore, these results suggested that CCS, as the anti-adhesion barrier, could effectively inhibit the postoperative intra-abdominal adhesion in rats partly through blocking TGF-β1 associated pathway and resulting in the degradation of collagen fibers at injured sites (Fig. 11).

The mechanistic studies of CCS as the anti-inflammatory drug on prevention of peritoneal adhesion were next assessed using surgical rats. It is known that at the early stage after peritoneal injury, inflammatory responses occur at traumatized sites, in which various proinflammatory factors (e.g. TGF-β1, TNF-α, IL-1β and IL-6) are released (Zhang et al., 2014). The mitogen-activated protein kinase (MAPK) inflammation signaling pathway has been reported to be activated by these proinflammatory cascades (Wang et al., 2017). As TGF-β1 and TNF-α were effectively suppressed by CCS (Fig. 5 and 9), it was not surprising to note that the activity of classic kinases in the MAPK signaling pathway such as TGF-β1-activating kinase (TAK1), c-Jun N-terminal kinase (JNK), and P38 mitogen-activated protein kinase (p38), was also inhibited (Fig. 10). It is also known that phosphorylation of TAK1 may act as the stimulus to induce the phosphorylation of JNK and p38, as a result for the transcription regulation of inflammation mediators and proinflammatory cytokines to promote systemic inflammation (Ayroldi et al., 2012). These results suggest that CCS, as the anti-inflammation drug, was able to inhibit inflammatory responses via downregulation of the MAPK signaling pathway, resulting in prevention of intra-abdominal adhesion (Fig. 11).

It is interesting to note that CCS in high dose achieved significantly better prevention results compared to CCS in low and middle doses (Fig. 1 and Table 1). However,

mechanistic studies of CCS as the anti-adhesion barrier demonstrated that the downregulation of TGF-β1, α-SMA and PAI-1 and the activation of tPA achieved by CCS in high dose were not significantly better than those obtained by CCS in low and middle doses (Fig. 5, 7 and 8). It was most likely that the PAI-1 expression can be regulated by different TGF-β1 associated signaling pathways such as Smads/p53 pathway (Kawarada et al., 2016), MEK/ERK pathway (Samarakoon et al., 2005), and YAP/TAZ pathway (Thomasy et al., 2013). In addition, the remodeling of the ECM that causes fibrotic tissue or scar due to collagen deposition in the skin has been found for wound healing (Philips et al., 2004). It is also known that metalloproteinases (MMPs, a family of proteases) are essential to the ECM remodeling process (Philips et al., 2004). It has been recently reported that TGF-β1 was able to impair the interaction of MMPs with their inhibitors (tissue inhibitor of matrix metalloproteinases, TIMPs), resulting in production of the ECM in injured tissues (Philips et al., 2004). Therefore, the influence of CCS on the cross-talk of these TGF-β associated signaling pathways, in order to improve the understanding of anti-adhesion effects (i.e. downregulation of fibrosis and promotion of fibrolysis), will be the focus of future work.

Similarly, mechanistic studies of CCS as the anti-inflammatory drug presented that CCS in high dose did not achieve significantly better reduction of TAK-1, JNK and p38 cascades compared to CCS in low and middle doses (Fig. 10). It has been reported that the activation of MAPK pathway can be also regulated by IL-1β and IL-6, causing inflammation within injured tissues (Wang et al., 2017). In addition to the MAPK pathway, inflammatory pathways such as NK-kB (Tsai et al., 2013)), MEK/ERK(Samarakoon et al., 2005) and RhoA/ROCK (Rao et al., 2017) are associated to the formation of intra-abdominal adhesion (Fig. 11). Therefore, the influence of CCS on these signaling cascades, with a hope to improve the understanding of anti-inflammation effects, will be investigated in future.

Prevention of postoperative intra-abdominal adhesion is mainly resulted from the

downregulation of fibrosis, promotion of fibrolysis, and inhibition of inflammatory response (Ambler et al., 2012) In this study, a combined prevention strategy using the co-administration of three natural materials (chitosan, cellulose and seaweed polysaccharide) resulted in additive anti-adhesion effects in rats with abdominal surgery. The resultant adhesion prevention was due to both anti-fibroblastic and anti-inflammatory effects. In addition, CCS did not cause any significant toxicity, as the animal body weights treated with CCS were similar to those of the untreated and sham groups (data not shown). As a result, CCS holds great therapeutic potential in the treatment of postoperative intra-abdominal adhesion.

Authorship Contributions

Participated in research design: L.Tian, J Pei.

Conducted experiments: L. Tian, H. Li, K. Liu, Y. Li, Y. Sun, Z. Cong, X.Luan, L.Wang, Z.Ren, D.Cong, H.Wang

Performed data analysis:L.Tian, Y. Li, J.Chen

Wrote or contributed to the writing of the manuscript:L. Tian,H. Li

References

Aarons CB, Cohen PA, Gower A, Reed KL, Leeman SE, Stucchi AF and Becker JM (2007) Statins (HMG-CoA reductase inhibitors) decrease postoperative adhesions by increasing peritoneal fibrinolytic activity. *Ann Surg* **245**:176-184.

Ambler DR, Fletcher NM, Diamond MP and Saed GM (2012) Effects of hypoxia on the expression of inflammatory markers IL-6 and TNF-a in human normal peritoneal and adhesion fibroblasts. *Syst Biol Reprod Med* **58**:324-329.

Ayroldi E, Cannarile L, Migliorati G, Nocentini G, Delfino DV and Riccardi C (2012) Mechanisms of the anti-inflammatory effects of glucocorticoids: genomic and nongenomic interference with MAPK signaling pathways. *The FASEB Journal* **26**:4805-4820.

Bi J, Zhang S, Du Z, Zhang J, Deng Y, Liu C and Zhang J (2017) Peripheral serotonin regulates postoperative intra-abdominal adhesion formation in mice. *Sci Rep* **7**:10001.

Cassidy MR, Sherburne AC, Sheldon HK, Gainsbury ML, Heydrick S and Stucchi AF (2014) Histone deacetylase inhibitors decrease intra-abdominal adhesions with one intraoperative dose by reducing peritoneal fibrin deposition pathways. *Surgery* **155**:234-244.

Chang J, Thunder R, Most D, Longaker MT and Lineaweaver WC (2000) Studies in flexor tendon wound healing: neutralizing antibody to TGF-beta1 increases postoperative range of motion. *Plast Reconstr Surg* **105**:148-155.

Chaturvedi AA, Lomme RM, Hendriks T and van Goor H (2014) Ultrapure alginate anti-adhesion gel does not impair colon anastomotic strength. *J Surg Res* **192**:432-439.

Chegini N, Kotseos K, Zhao Y, Bennett B, McLean FW, Diamond MP, Holmdahl L and Burns J (2001) Differential expression of TGF-beta1 and TGF-beta3 in serosal tissues of human intraperitoneal organs and peritoneal adhesions. *Hum Reprod* **16**:1291-1300.

Daroz LR, Lopes JB, Dallan LA, Campana-Filho SP, Moreira LF and Stolf NA (2008) Prevention of postoperative pericardial adhesions using thermal sterile carboxymethyl chitosan. *Rev Bras Cir Cardiovasc* **23**:480-487.

Deng L, Li Q, Lin G, Huang D, Zeng X, Wang X, Li P, Jin X, Zhang H, Li C, Chen L, Wang L, Huang S, Shao H, Xu B and Mao J (2016) P-glycoprotein Mediates Postoperative Peritoneal Adhesion Formation by Enhancing Phosphorylation of the Chloride Channel-3. *Theranostics* **6**:204-218.

Esposito AJ, Heydrick SJ, Cassidy MR, Gallant J, Stucchi AF and Becker JM (2013) Substance P is an early mediator of peritoneal fibrinolytic pathway genes and promotes intra-abdominal adhesion formation. *J Surg Res* **181**:25-31.

Fotiadis K, Filidou E, Arvanitidis K, Valatas V, Stavrou G, Basdanis G, Paspaliaris V, Kolios G and Kotzampassi K (2015) Intraperitoneal application of phospholipids for the prevention of postoperative adhesions: a possible role of myofibroblasts. *J Surg Res* **197**:291-300.

Francesko A and Tzanov T (2011) Chitin, chitosan and derivatives for wound healing and tissue engineering. *Adv Biochem Eng Biotechnol* **125**:1-27.

Gomel V, Urman B and Gurgan T (1996) Pathophysiology of adhesion formation and strategies for prevention. *J Reprod Med* **41**:35-41.

Guo J, Ogier JR, Desgranges S, Darcy R and O'Driscoll C (2012) Anisamide-targeted cyclodextrin nanoparticles for siRNA delivery to prostate tumours in mice. *Biomaterials* **33**:7775-7784.

Guo J, Russell EG, Darcy R, Cotter TG, McKenna SL, Cahill MR and O'Driscoll CM (2017) Antibody-Targeted Cyclodextrin-Based Nanoparticles for siRNA Delivery in the Treatment of Acute Myeloid Leukemia: Physicochemical Characteristics, in Vitro Mechanistic Studies, and ex Vivo Patient Derived Therapeutic Efficacy. *Mol Pharm* **14**:940-952.

Holmdahl L, Kotseos K, Bergstrom M, Falk P, Ivarsson ML and Chegini N (2001) Overproduction of transforming growth factor-beta1 (TGF-beta1) is associated with adhesion formation and peritoneal fibrinolytic impairment. *Surgery* **129**:626-632.

Honjo K, Munakata S, Tashiro Y, Salama Y, Shimazu H, Eiamboonsert S, Dhahri D, Ichimura A, Dan T, Miyata T, Takeda K, Sakamoto K, Hattori K and Heissig B (2017) Plasminogen activator inhibitor-1 regulates macrophage-dependent postoperative adhesion by enhancing EGF-HER1 signaling in mice. *FASEB J* **31**:2625-2637.

Hu J, Fan D, Lin X, Wu X, He X, He X, Wu X and Lan P (2015) Safety and Efficacy of Sodium Hyaluronate Gel and Chitosan in Preventing Postoperative Peristomal Adhesions After Defunctioning Enterostomy: A Prospective Randomized Controlled Trials. *Medicine (Baltimore)* **94**:e2354.

Kawarada Y, Inoue Y, Kawasaki F, Fukuura K, Sato K, Tanaka T, Itoh Y and Hayashi H (2016) TGF-beta induces p53/Smads complex formation in the PAI-1 promoter to activate transcription. *Sci Rep* **6**:35483.

Ko W, Sohn JH, Jang JH, Ahn JS, Kang DG, Lee HS, Kim JS, Kim YC and Oh H (2016) Inhibitory effects of alternaramide on inflammatory mediator expression through TLR4-MyD88-mediated inhibition of NF-small ka, CyrillicB and MAPK pathway signaling in lipopolysaccharide-stimulated RAW264.7 and BV2 cells. *Chem Biol Interact* **244**:16-26.

Liakakos T, Thomakos N, Fine PM, Dervenis C and Young RL (2001) Peritoneal adhesions: etiology, pathophysiology, and clinical significance. Recent advances in prevention and management. *Dig Surg* **18**:260-273.

Lou W, Zhang H, Ma J, Zhang D, Liu C, Wang S, Deng Z, Xu H and Liu J (2012) In vivo evaluation of in situ polysaccharide based hydrogel for prevention of postoperative adhesion. *Carbohydr Polym* **90**:1024-1031.

Nair SK, Bhat IK and Aurora AL (1974) Role of proteolytic enzyme in the prevention of postoperative intraperitoneal adhesions. *Arch Surg* **108**:849-853.

Parsak CK, Satar S, Akcam T, Satar D and Sungur I (2007) Effectiveness of treatment to prevent adhesions after abdominal surgery: an experimental evaluation in rats. *Adv Ther* **24**:796-802.

Philips N, Keller T and Gonzalez S (2004) TGF beta-like regulation of matrix metalloproteinases by anti-transforming growth factor-beta, and anti-transforming growth factor-beta 1 antibodies in dermal fibroblasts: Implications for wound healing. *Wound Repair Regen* **12**:53-59.

Poehnert D, Grethe L, Maegel L, Jonigk D, Lippmann T, Kaltenborn A, Schrem H, Klempnauer J and Winny M (2016) Evaluation of the Effectiveness of Peritoneal Adhesion Prevention Devices in a Rat Model. *Int J Med Sci* **13**:524-532.

Rao J, Ye Z, Tang H, Wang C, Peng H, Lai W, Li Y, Huang W and Lou T (2017) The RhoA/ROCK Pathway Ameliorates Adhesion and Inflammatory Infiltration Induced by AGEs in Glomerular Endothelial Cells. *Sci Rep* **7**:39727.

Reed KL, Fruin AB, Gower AC, Stucchi AF, Leeman SE and Becker JM (2004) A neurokinin 1 receptor antagonist decreases postoperative peritoneal adhesion formation and increases peritoneal fibrinolytic activity. *P Natl Acad Sci USA* **101**:9115-9120.

Risberg B (1997) Adhesions: preventive strategies. *Eur J Surg Suppl*:32-39.

Rocha HA, Franco CR, Trindade ES, Carvalho LC, Veiga SS, Leite EL, Dietrich CP and Nader HB (2001) A fucan from the brown seaweed Spatoglossum schroederi inhibits Chinese hamster ovary cell adhesion to several extracellular matrix proteins. *Braz J Med Biol Res* **34**:621-626.

Ryan CK and Sax HC (1995) Evaluation of a carboxymethylcellulose sponge for prevention of postoperative adhesions. *Am J Surg* **169**:154-159; discussion 159-160.

Samarakoon R, Higgins CE, Higgins SP, Kutz SM and Higgins PJ (2005) Plasminogen activator inhibitor type-1 gene expression and induced migration in TGF-beta1-stimulated smooth muscle cells is pp60(c-src)/MEK-dependent. *J Cell Physiol* **204**:236-246.

Sanjeewa KKA, Kim EA, Son KT and Jeon YJ (2016) Bioactive properties and potentials cosmeceutical applications of phlorotannins isolated from brown seaweeds: A review. *J Photochem Photobiol B* **162**:100-105.

Shao W, Wu J, Liu H, Ye S, Jiang L and Liu X (2017) Novel bioactive surface functionalization of bacterial cellulose membrane. *Carbohydr Polym* **178**:270-276.

Thomasy SM, Morgan JT, Wood JA, Murphy CJ and Russell P (2013) Substratum stiffness and latrunculin B modulate the gene expression of the mechanotransducers YAP and TAZ in human trabecular meshwork cells. *Exp Eye Res* **113**:66-73.

Tsai SH, Huang PH, Peng YJ, Chang WC, Tsai HY, Leu HB, Chen JW and Lin SJ (2013) Zoledronate attenuates angiotensin II-induced abdominal aortic aneurysm through inactivation of Rho/ROCK-dependent JNK and NF-kappaB pathway. *Cardiovasc Res* **100**:501-510.

Wang K, Wang F, Bao JP, Xie ZY, Chen L, Zhou BY, Xie XH and Wu XT (2017) Tumor necrosis factor alpha modulates sodium-activated potassium channel SLICK in rat dorsal horn neurons via p38 MAPK activation pathway. *J Pain Res* **10**:1265-1271.

Wei G, Chen X, Wang G, Jia P, Xu Q, Ping G, Wang K and Li X (2015) Inhibition of cyclooxygenase-2 prevents intra-abdominal adhesions by decreasing activity of peritoneal fibroblasts. *Drug Des Devel Ther* **9**:3083-3098.

Wei G, Wu Y, Gao Q, Zhou C, Wang K, Shen C, Wang G, Wang K, Sun X and Li X (2017) Effect of Emodin on Preventing Postoperative Intra-Abdominal Adhesion Formation. *Oxid Med Cell Longev* **2017**:1740317.

Yang B, Gong C, Zhao X, Zhou S, Li Z, Qi X, Zhong Q, Luo F and Qian Z (2012) Preventing postoperative abdominal adhesions in a rat model with PEG-PCL-PEG hydrogel. *Int J Nanomedicine* **7**:547-557.

Yang Y, Yang S, Chen M, Zhang X, Zou Y and Zhang X (2008) Compound Astragalus and Salvia miltiorrhiza Extract exerts anti-fibrosis by mediating TGF-beta/Smad signaling in myofibroblasts. *J Ethnopharmacol* **118**:264-270.

Zhang Y, Li X, Zhang Q, Li J, Ju J, Du N, Liu X, Chen X, Cheng F, Yang L, Xu C, Bilal MU, Wei Y, Lu Y and Yang B (2014) Berberine hydrochloride prevents postsurgery intestinal adhesion and inflammation in rats. *J Pharmacol Exp Ther* **349**:417-426.

Zheng Z, Zhang W, Sun W, Li X, Duan J, Cui J, Feng Z and Mansour HM (2013) Influence of the carboxymethyl chitosan anti-adhesion solution on the TGF-beta1 in a postoperative peritoneal adhesion rat. *J Mater Sci Mater Med* **24**:2549-2559.

Zhu L, Peng L and Zhang YQ (2015) The processing of chitosan and its derivatives and their application for postoperative anti-adhesion. *Mini Rev Med Chem* **15**:330-337.

Footnotes

This work was supported by the Jilin Province Development and Reform Commission (Grant No.2014N149) and Jilin Department of Science and Technology (Grant No. 20160209013YY).

Legends for figures

Fig.1 Intra-abdominal adhesions (red triangle) in rats on Day14 after surgery (n = 10). No adhesion was observed in the untreated and sham groups, in which the surfaces of the parietal peritoneum and cecum were smooth. Obvious adhesions were formed in model group treated with saline. Adhesions in groups of CS (10 mg/ml) and CL (6 mg/ml) were clearly less than in the model group and the CC group (8 mg/ml). CCS with high dose achieved effective anti-adhesion results compared to CCS with low and middle doses.

Fig.2. The collagen deposition and fibrosis were demonstrated using Masson Trichrome staining (red tetragonum) in tissues with adhesion (n=4) (100x magnification). (Collagen fibers and mucosa: blue; muscle fiber and cellulose: red).

Fig.3. The fibrosis in the intra-abdominal adhesions was demonstrated using Picrosirius Red staining (black tetragonum) (n=4) (100x magnification pictures).

Fig.4. Hematoxylin-Eosin staining of injured tissues (n=4). Black tetragonum represented the accumulation of plasma cells, granulocytes, and macrophages. Red circle represented the vascular proliferation and congestion. (200x magnification).

Fig.5 The expression of TGF-β1 mRNA (A) and protein (B) in injured peritoneal tissues. (A) TGF-β1 mRNA level in cecum of rats was assessed using RT-qPCR. Compared with the model group (saline), the expression of TGF-β1 mRNA in CS, CL and CC were significantly decreased (P<0.05). In addition, the TGF-β1 mRNA level in CCS with high dose was significantly suppressed compared to CS, CL and CC groups (P<0.05). (B) TGF-β1 protein level in serum was evaluated using ELISA. The level of TGF-β1 protein in CCS with high dose was also significantly suppressed compared to CS, CL and CC. Values were presented as mean ± standard deviation from 6 animals in each group. $^{\#}P$<0.05, compared with CS, CL and CC; *P<0.05, compared with the model group (saline).

Fig.6 The expression of TGF-β1 was demonstrated using IHC in tissues with adhesion (n=4). (200x magnification).

Fig.7 The expression of α-SMA protein was assessed using western blot. (A) A representative image presented that CCS with three doses effectively reduced the expression of α-SMA protein. (B) In addition, CCS with high dose significantly downregulated the α-SMA protein compared to CS, CL and CC (mean ± standard deviation from 4 animals in nine groups). $^{\#}P$<0.05, compared with CS, CL and CC; *P<0.05, compared with the model group (saline); **P<0.05, compared with the model group (saline).

Fig.8 The mRNA and protein levels of PAI-1 and tPA in injured peritoneal tissues were assessed using RT-qPCR and ELISA. The expression of PAI-1 mRNA (A) and protein (B) were effectively suppressed with CCS in three doses. Following the downregulation of PAI-1, the expression of tPA mRNA (C) and protein (D) was significantly increased with CCS (high dose) compared to CS, CL and CC. Values were shown as mean ± standard deviation (n=6). $^{\#}P<0.05$, compared with CS, CL and CC; $*P<0.05$, compared with the model group (saline).

Fig.9 The mRNA and protein levels of inflammatory cytokine TNF-α in serum were assessed using RT-qPCR (A) and ELSIA (B), respectively. The results were presented as mean ± standard deviation (n=6). $^{\#}P<0.05$, compared with CS, CL and CC; $*P<0.05$, compared with the model group (saline).

Fig.10 The activity of TAK1, JNK and p38 in intra-abdominal adhesions was confirmed using western blot. The expression of (B) TAK-1, (D) JNK and (F) p38 was not significantly varied between the treatments. However, the phosphorylation of (C) TAK-1, (E) JNK and (G) p38 was significantly inactivated using CCS. $^{\#}P<0.05$, compared with CS, CL and CC; $*P<0.05$, compared with the model group (saline); $**P<0.05$, compared with the model group (saline). Mean ± standard deviation (n=4).

Fig. 11 CCS may induce both anti-fibrosis and anti-inflammatory effects, potentially inhibiting the postoperative intra-abdominal adhesion.Anti-fibrosis effects: the expression of plasminogen activator inhibitor-1 (PAI-1, a key factor for the adhesion formation) can be regulated by different TGF-β1 associated signaling pathways such as Smads/p53 pathway, MMP/TIMPS pathway, MEK/ERK pathway, and YAP/TAZ pathway. Following the downregulation of PAI-1 achieved by CCS, the activation of tissue plasminogen activator (tPA, may generate plasmin that is a fibrinolytic factor capable of breaking down fibrin) is significantly promoted. Anti-inflammation effects: CCS may suppress the Phosphorylation of classic kinases (e.g. TAK1, JNK and p38) in the MAPK signaling pathway. In addition to the MAPK pathway, inflammatory pathways such as NK-kB, MEK/ERK and RhoA/ROCK, are associated to the formation of intra-abdominal adhesion. Therefore, the prevention mechanisms of CCS will be further investigated in future, with a hope of fully understanding of anti-adhesion effects.

JPET Fast Forward. Published on December 20, 2017 as DOI: 10.1124/jpet.117.244400
This article has not been copyedited and formatted. The final version may differ from this version.

Table 1. Scores of abdominal adhesion on Day 14 after surgery.
Median of adhesion scores represented the severity of adhesion in the untreated group, sham group, the model groups treated with CS (10mg/ml), CL (6mg/ml), CC (8mg/ml), CCS in three doses (n=10). Comparisons between different groups were applied using the Kruskal-Wallis H and Mann-Whitney U tests (SPSS 15.0). *$P<0.05$, compared with the model group (saline); $^{\#}P<0.05$, compared with CS, CL and CC.

Groups（n=10）	Adhesion Score					Median Score
	0	Ⅰ	Ⅱ	Ⅲ	Ⅳ	
Untreated	10	0	0	0	0	0
Sham	10	0	0	0	0	0
Model+Saline	0	0	1	1	8	4
Model+CS	0	1	4	3	2	2.5*
Model+CL	1	1	3	2	3	2.5*
Model+CC	0	2	2	3	3	3
Model+CCS (Low dose)	1	1	3	3	2	2.5*
Model+CCS (Middle dose)	2	2	2	1	3	2*
Model+CCS (High dose)	2	1	3	4	0	2*#

JPET Fast Forward. Published on December 20, 2017 as DOI: 10.1124/jpet.117.244400
This article has not been copyedited and formatted. The final version may differ from this version.

Fig.1

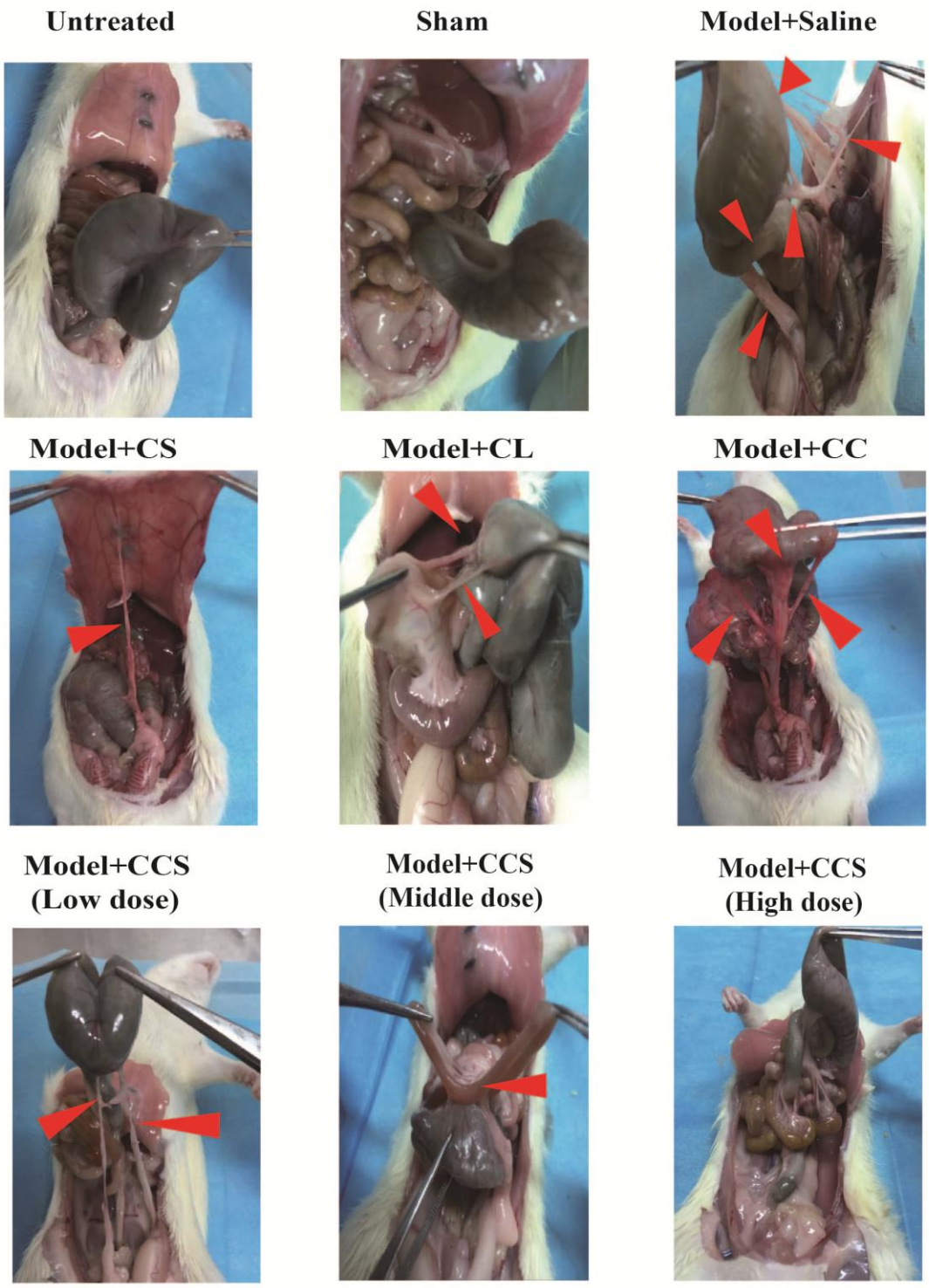

JPET Fast Forward. Published on December 20, 2017 as DOI: 10.1124/jpet.117.244400
This article has not been copyedited and formatted. The final version may differ from this version.

Fig.2

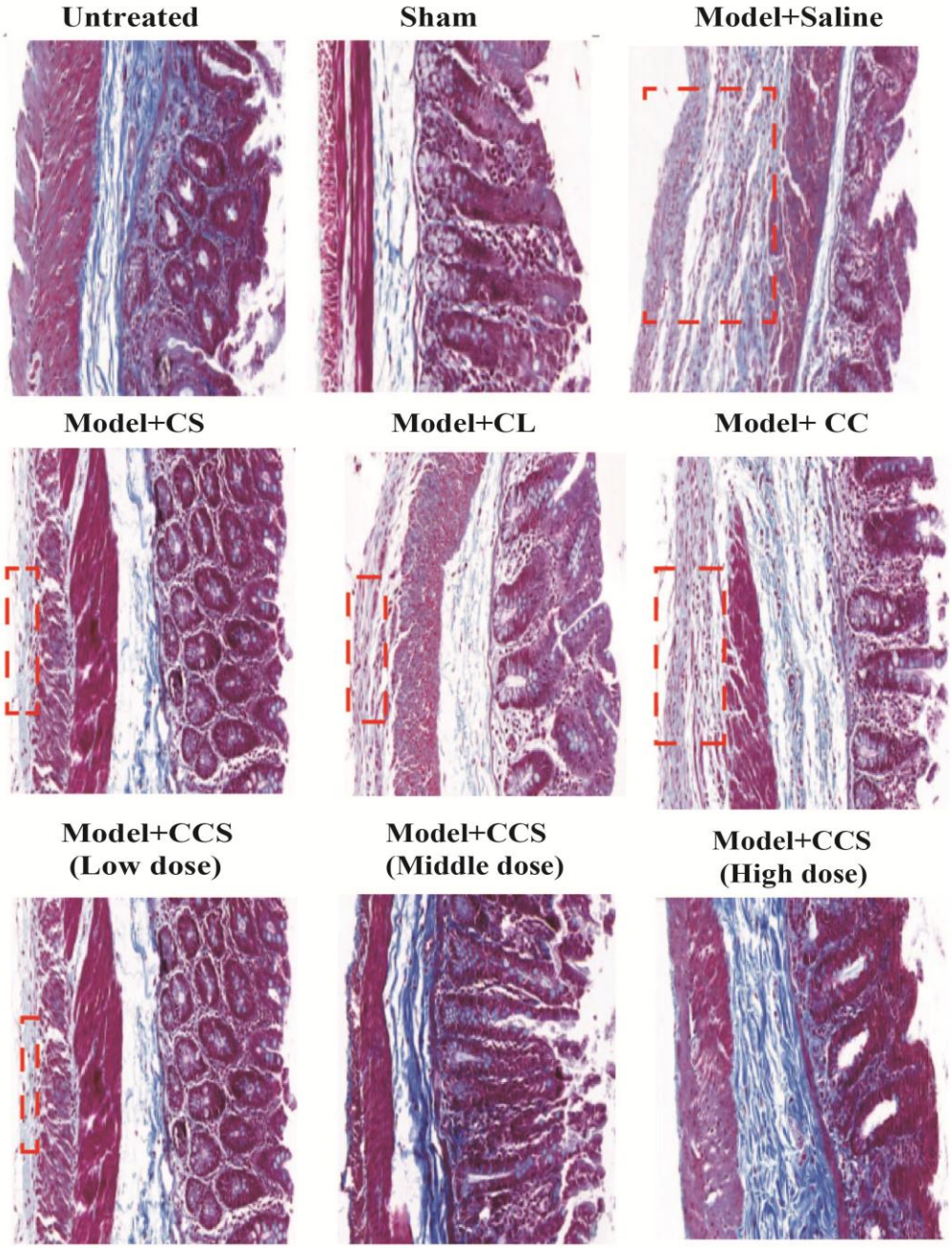

JPET Fast Forward. Published on December 20, 2017 as DOI: 10.1124/jpet.117.244400
This article has not been copyedited and formatted. The final version may differ from this version.

Fig.3

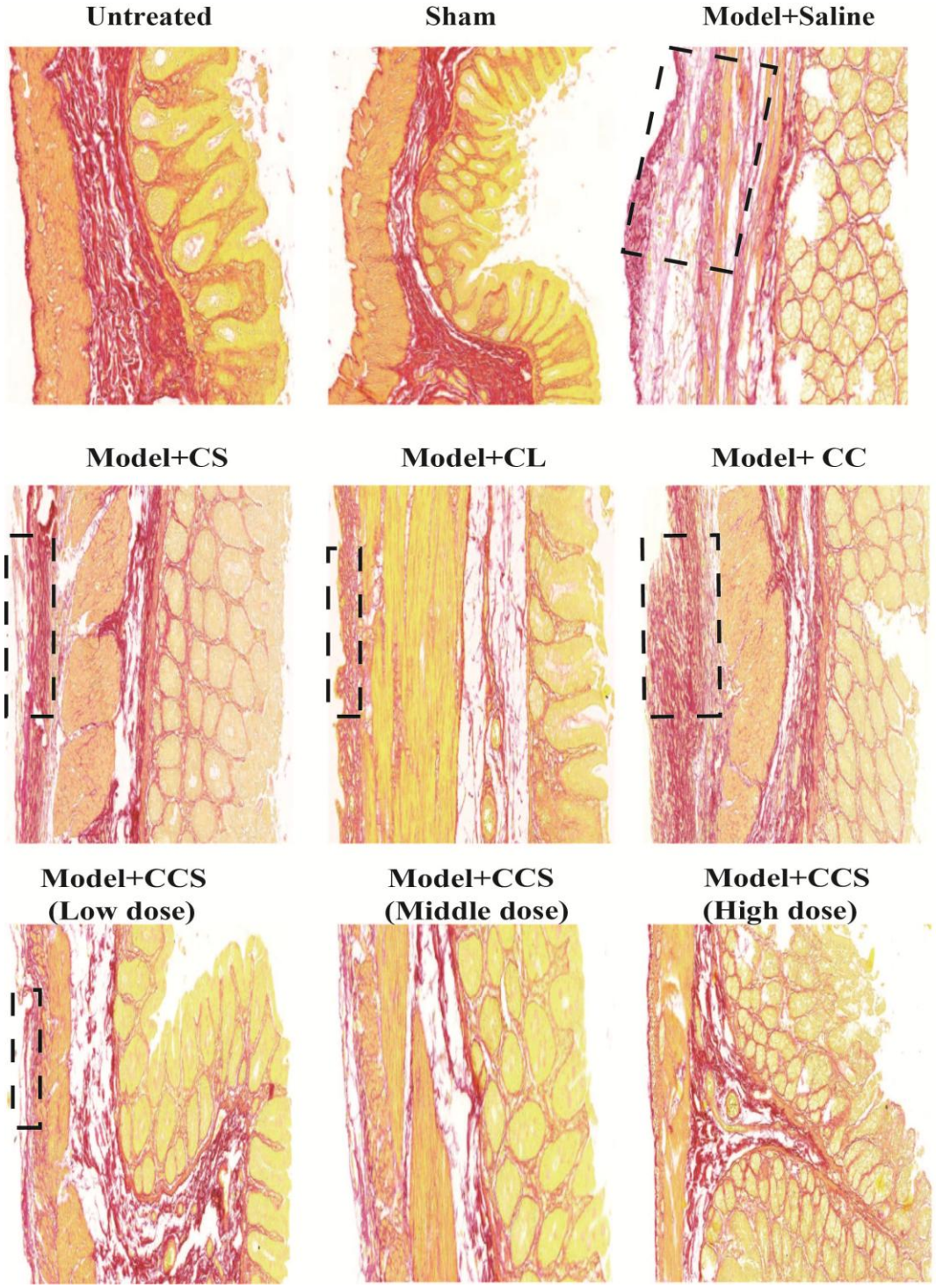

JPET Fast Forward. Published on December 20, 2017 as DOI: 10.1124/jpet.117.244400
This article has not been copyedited and formatted. The final version may differ from this version.

Fig.4

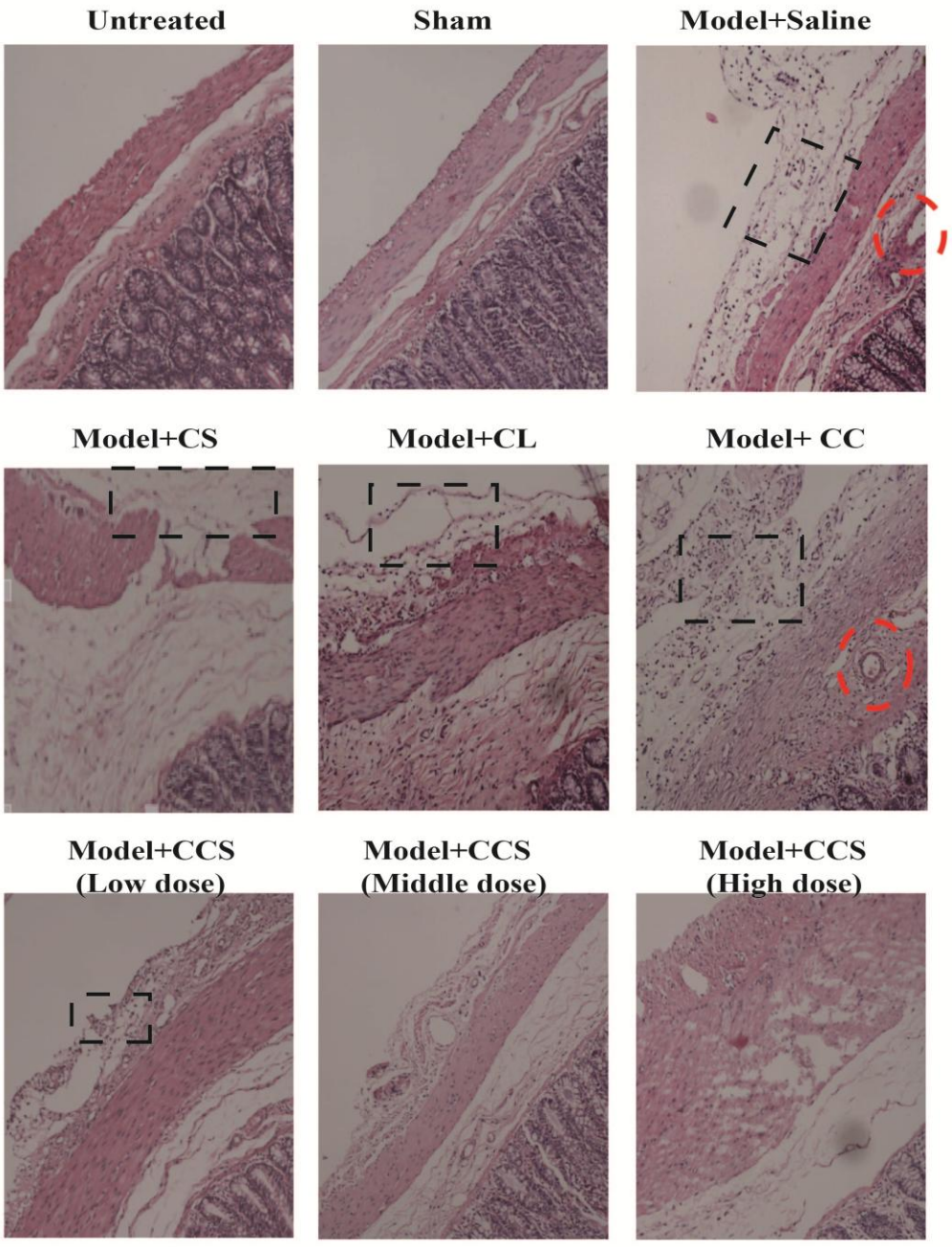

JPET Fast Forward. Published on December 20, 2017 as DOI: 10.1124/jpet.117.244400
This article has not been copyedited and formatted. The final version may differ from this version.

Fig.5

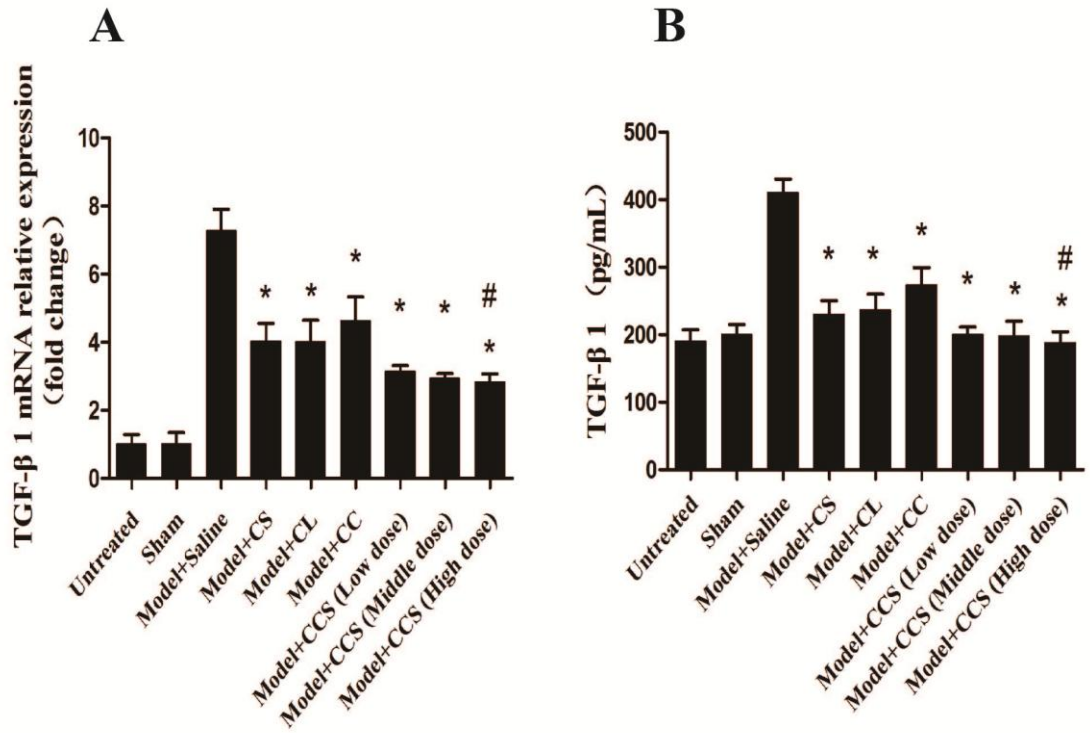

JPET Fast Forward. Published on December 20, 2017 as DOI: 10.1124/jpet.117.244400
This article has not been copyedited and formatted. The final version may differ from this version.

Fig.6

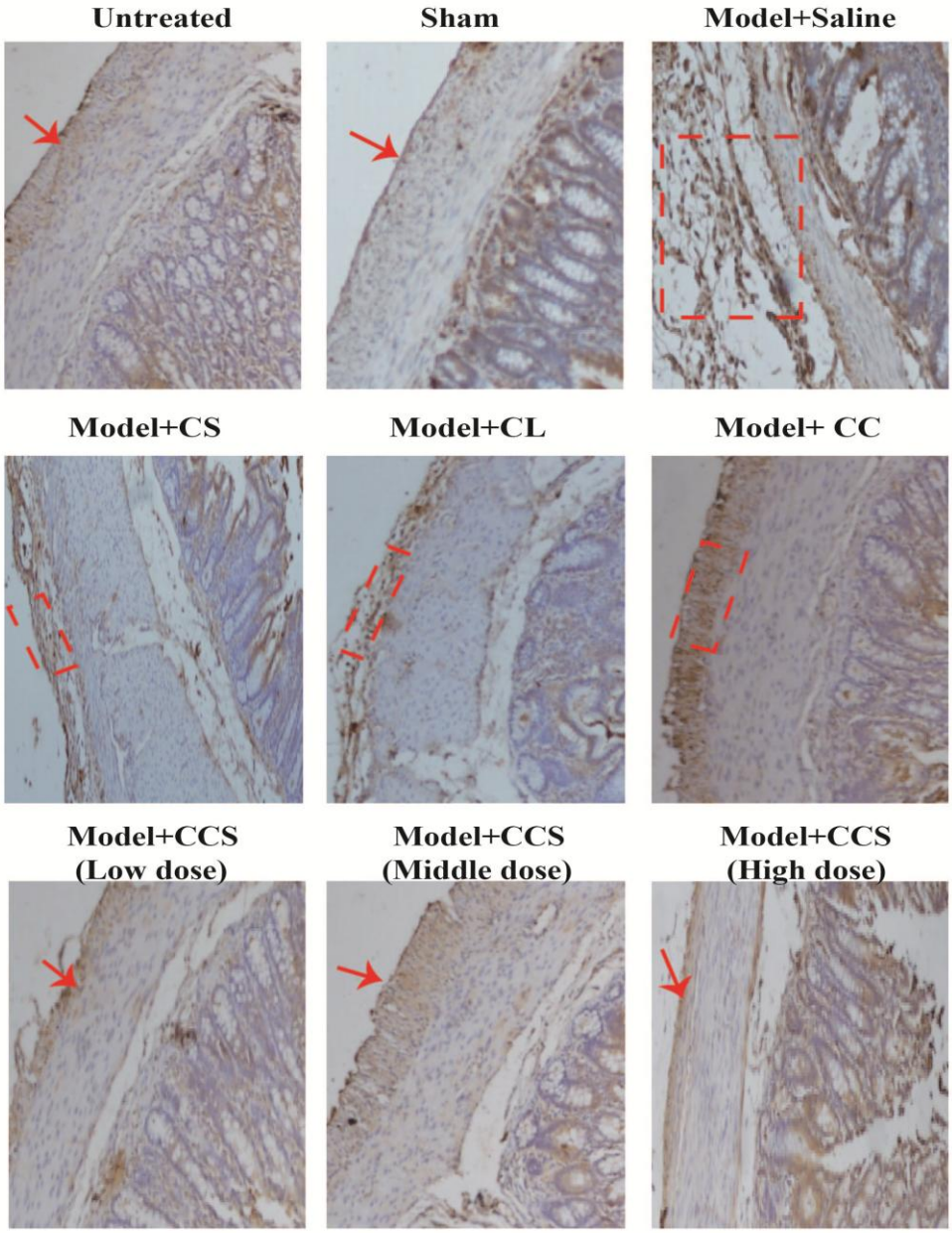

JPET Fast Forward. Published on December 20, 2017 as DOI: 10.1124/jpet.117.244400
This article has not been copyedited and formatted. The final version may differ from this version.

Fig.7

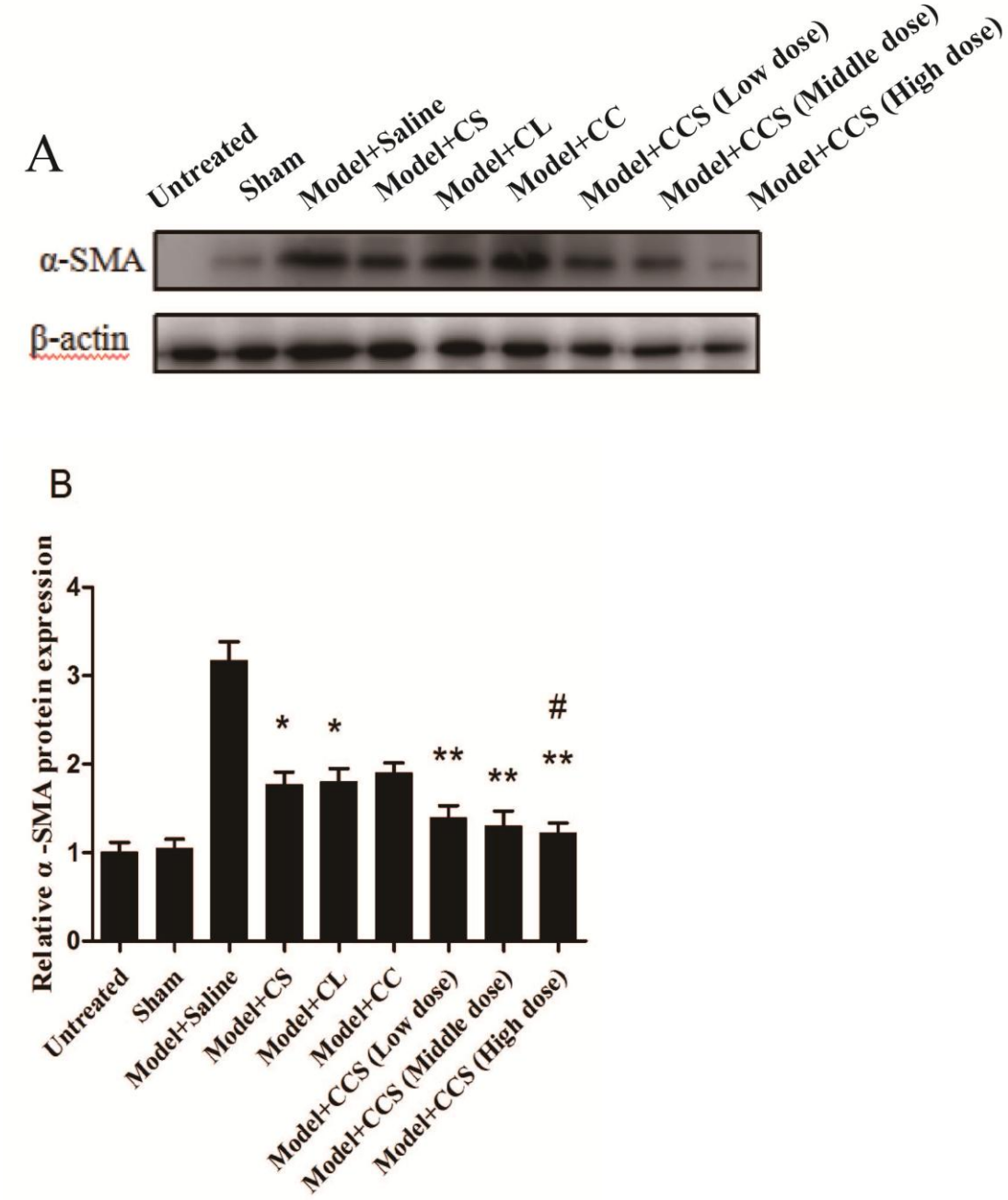

Fig.8

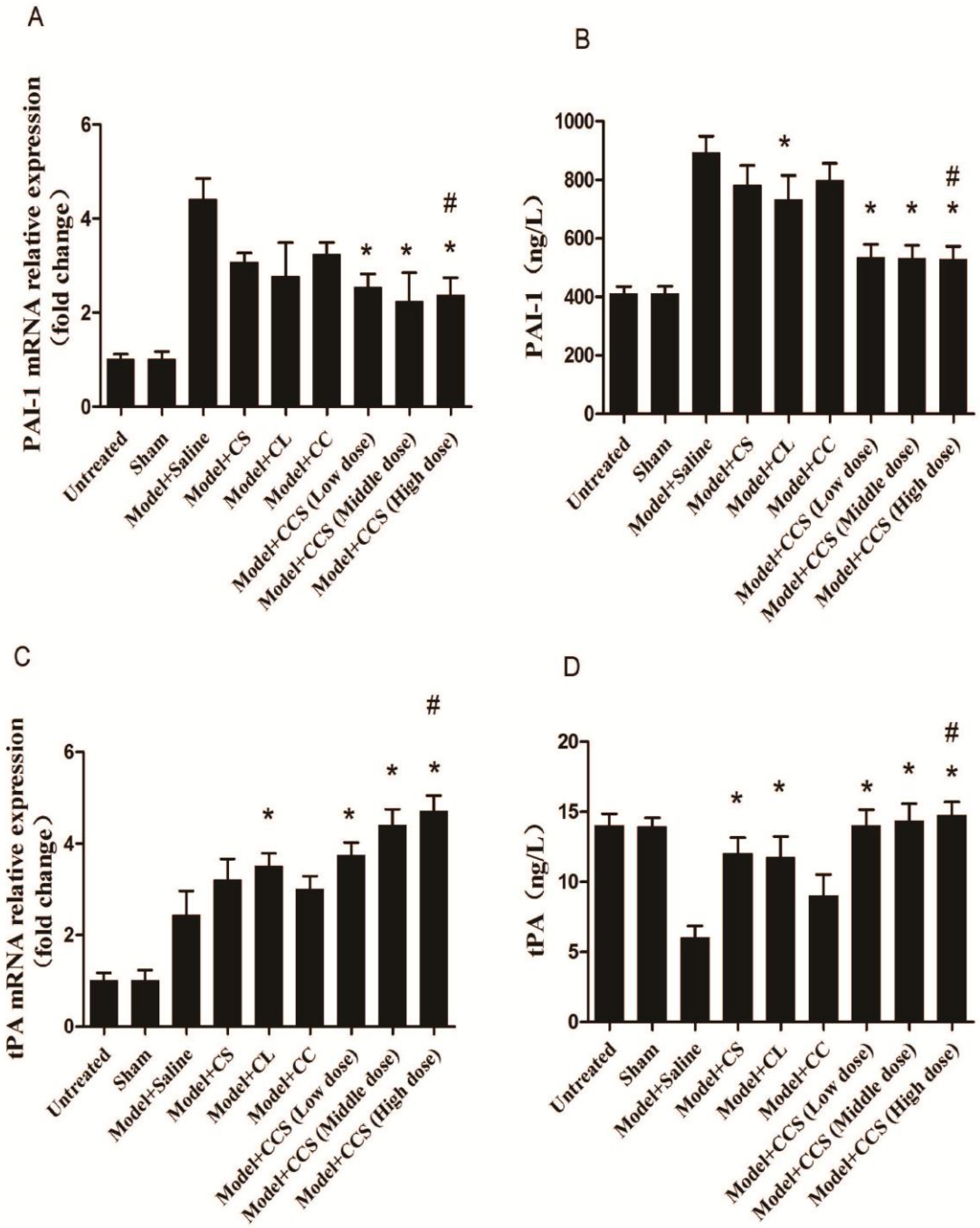

JPET Fast Forward. Published on December 20, 2017 as DOI: 10.1124/jpet.117.244400
This article has not been copyedited and formatted. The final version may differ from this version.

Fig.9

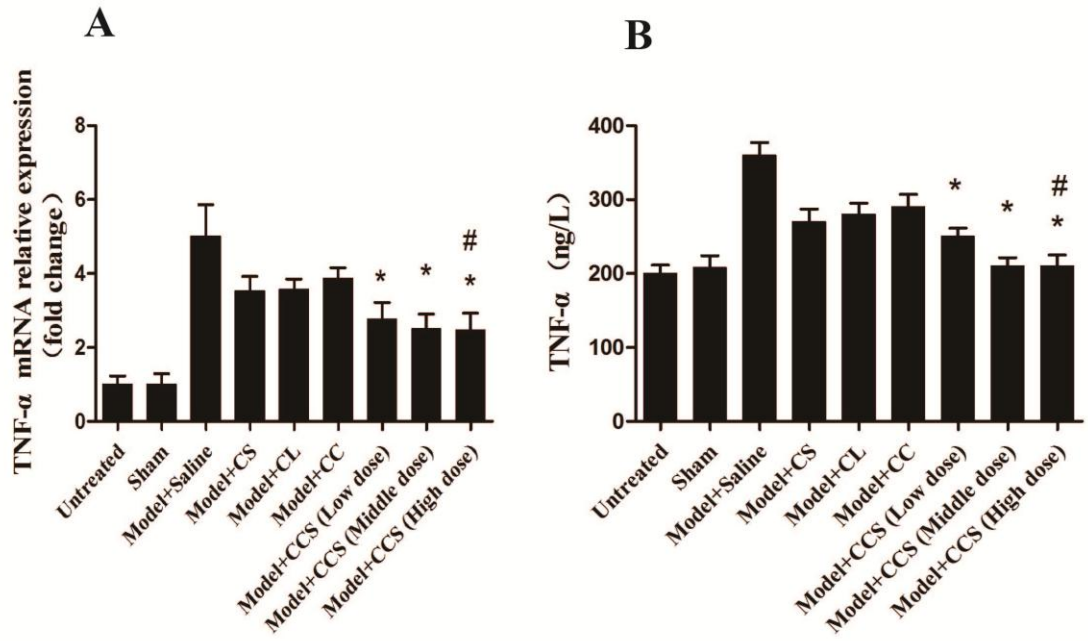

JPET Fast Forward. Published on December 20, 2017 as DOI: 10.1124/jpet.117.244400
This article has not been copyedited and formatted. The final version may differ from this version.

Fig.10

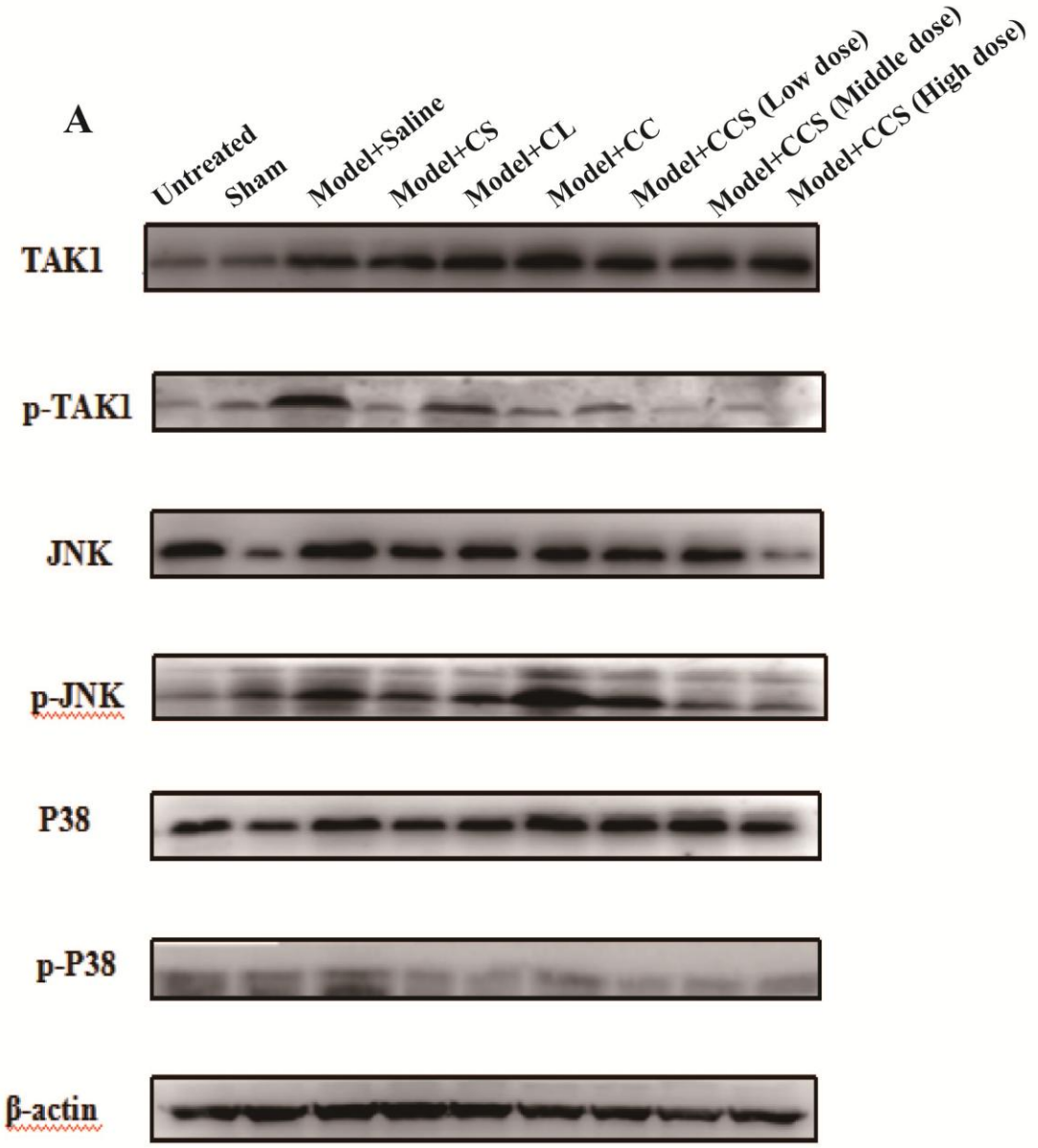

JPET Fast Forward. Published on December 20, 2017 as DOI: 10.1124/jpet.117.244400
This article has not been copyedited and formatted. The final version may differ from this version.